

## Nanorheology of Entangled Polymer Melts

Ting Ge,<sup>1,†</sup> Gary S. Grest,<sup>2</sup> and Michael Rubinstein<sup>1,\*†</sup>

<sup>1</sup>*Department of Chemistry, University of North Carolina, Chapel Hill, North Carolina 27599, USA*

<sup>2</sup>*Sandia National Laboratories, Albuquerque, New Mexico 87185, USA*

 (Received 27 June 2017; revised manuscript received 17 October 2017; published 1 February 2018)

We use molecular simulations to probe the local viscoelasticity of an entangled polymer melt by tracking the motion of embedded nonsticky nanoparticles (NPs). As in conventional microrheology, the generalized Stokes-Einstein relation is employed to extract an effective stress relaxation function  $G_{\text{GSE}}(t)$  from the mean square displacement of NPs.  $G_{\text{GSE}}(t)$  for different NP diameters  $d$  are compared with the stress relaxation function  $G(t)$  of a pure polymer melt. The deviation of  $G_{\text{GSE}}(t)$  from  $G(t)$  reflects the incomplete coupling between NPs and the dynamic modes of the melt. For linear polymers, a plateau in  $G_{\text{GSE}}(t)$  emerges as  $d$  exceeds the entanglement mesh size  $a$  and approaches the entanglement plateau in  $G(t)$  for a pure melt with increasing  $d$ . For ring polymers, as  $d$  increases towards the spanning size  $R$  of ring polymers,  $G_{\text{GSE}}(t)$  approaches  $G(t)$  of the ring melt with no entanglement plateau.

DOI: 10.1103/PhysRevLett.120.057801

Microrheology is a powerful technique to measure the viscoelasticity of a medium through tracking the motion of embedded probe particles [1]. The particles are often much larger than any structural length scale of the medium, and their motion is coupled to the bulk viscoelasticity [2–4]. In this Letter, we use molecular simulations to explore the extension of microrheology to nanorheology, in which nanoparticles (NPs) smaller than or comparable to the structural length scales of the medium are used instead of micron-size beads. Specifically, we study NPs in a melt of entangled polymers. A key question is how viscoelastic modes of the melt affect the NP motion and how it is related to the diameter  $d$  of NPs and the structural length scales of the polymer melt, such as the average spacing  $a$  between polymer entanglements and the average size  $R$  of polymers.

Diffusion of NPs in a polymer melt is an essential process during the fabrication of polymer nanocomposites, a prominent class of hybrid materials [5,6]. Experiments [7–10] and simulations [6,11–13] have demonstrated that NP diffusion in a melt of entangled linear polymers depends on the relation between  $d$  and  $a$ . The mobility of NPs with  $d < a$  is higher than the prediction of the Stokes-Einstein relation [12,13]. Scaling theory [14] argues that these NPs are coupled only to the unentangled dynamics of local chain segments with sizes up to  $\approx d$ . The mobility of NPs with  $d > a$  is suppressed due to the confinement of the entanglement network [12,13]. While sufficiently large NPs are trapped by the network and cannot freely diffuse until the terminal relaxation of the network, NPs with  $d$  moderately larger than  $a$  can overcome the entanglement confinement through the hopping diffusion mechanism [15].

Recently, NP diffusion in an entangled melt of nonconcatenated ring polymers has also been studied using

simulations and scaling theory [13]. The motion of NPs with  $d > a$  in ring polymers is not as strongly suppressed as in linear polymers of the same lengths, as there is no entanglement network in a ring polymer melt. The comparison of NP diffusion in entangled linear chains and nonconcatenated rings exemplifies the effects of polymer architecture on the dynamical coupling between NPs and polymer melts.

One measure of viscoelasticity is the stress relaxation modulus  $G(t)$  as a function of time  $t$ . In microrheology,  $G(t)$  is linked to the mean squared displacement (MSD) of tracer particles  $\langle \Delta r^2(t) \rangle$  through the generalized Stokes-Einstein (GSE) relation [1,2]. In the domain of Laplace frequency  $s$ , the GSE relation is

$$\tilde{G}(s) = \frac{6k_B T}{f \pi d s \langle \Delta r^2(s) \rangle}, \quad (1)$$

in which  $\tilde{G}(s)$  and  $\widetilde{\Delta r^2}(s)$  are the unilateral Laplace transforms of  $G(t)$  and  $\langle \Delta r^2(t) \rangle$ , respectively.  $f = 3$  or  $2$ , depending on whether the particle-medium boundaries are stick or slip.

We employ the GSE relation to convert the simulation data of a NP MSD in a polymer melt to an effective stress relaxation function  $G_{\text{GSE}}(t)$ . The results of  $G_{\text{GSE}}(t)$  for NPs with different diameters  $d$  are compared with the stress relaxation function of the corresponding pure polymer melt  $G_{\text{GK}}(t)$ , which is obtained using the Green-Kubo formula. This comparison is performed for NPs in entangled linear polymers and nonconcatenated ring polymers. Through this comparison, we examine the coupling between NP motion and the bulk melt viscoelasticity and the dependence of the coupling on  $d$ .

The models of polymers and NPs are similar to those in previous molecular dynamics simulations [6,12,13,16–19].

Lennard-Jones units  $\sigma$ ,  $m$ , and  $\epsilon$  are used for the length, mass, and energy, respectively. For the entangled linear polymer melt, the number of monomers per entanglement strand  $N_e \approx 28$  [20,21], the average spacing between entanglements  $a \approx 5\sigma$  [21], and the entanglement time  $\tau_e \approx 4000\tau$  [22] with  $\tau = \sigma\sqrt{m/\epsilon}$ . The number of monomers in a polymer is  $N = 800$  for both linear chains and rings. NP diameter  $d$  ranges from  $3\sigma < a$  to  $15\sigma \approx 3a$ , and the volume fraction of NPs  $\phi_{\text{NP}} \approx 10\%$ . Previous simulations [6] have shown that the viscosity of a NP linear polymer composite is reduced with respect to that of the corresponding pure polymer melt if  $d < a$  and almost unchanged if  $d \approx a$ , while enhanced if  $d > a$ . The relative change of composite viscosity with respect to the pure melt viscosity can be up to  $\approx 25\%$  at  $\phi_{\text{NP}} \approx 10\%$ . For NP-ring systems, our simulation results show that the composite viscosity at  $\phi_{\text{NP}} \approx 10\%$  also changes by up to  $\approx 25\%$  depending on  $d$ . All samples were equilibrated at pressure  $P = 0$  and temperature  $T = 1.0\epsilon/k_B$ . Subsequent simulations were run at constant volume  $V$  for up to  $10^8\tau$ . MSDs  $\langle \Delta r^2(t) \rangle$  of NPs in the simulations have been reported in a previous paper [13]. Additional simulation details are presented in Supplemental Material [23].

The stress relaxation modulus for a pure polymer melt is calculated using the Green-Kubo formula

$$G_{\text{GK}}^{ij}(t) = \frac{V}{k_B T} \langle \overline{\sigma^{ij}(t)} \overline{\sigma^{ij}(0)} \rangle, \quad (2)$$

where  $\overline{\sigma^{ij}(t)}$  is the preaveraged stress [24] and  $i$  and  $j$  are Cartesian indices with  $i \neq j$ .  $G_{\text{GK}}(t)$  is computed as the average of  $G_{\text{GK}}^{ij}(t)$  with  $ij = xy, xz, \text{ and } yz$ .

We use the GSE relation [Eq. (1)] to convert  $\langle \Delta r^2(t) \rangle$  to  $G_{\text{GSE}}(t)$ . The conversion is done using the method developed by Mason [25]. One example of the conversion is given in Fig. 1. The early-time part of  $\langle \Delta r^2(t) \rangle$  is excluded from the conversion, as the inertialess GSE relation [Eq. (1)] is not applicable to the regime of ballistic motion and the subsequent crossover to thermal motion [26]. As shown in the inset in Fig. 1, a typical MSD curve starts with a ballistic regime where the log-log slope  $\alpha = d \log \langle \Delta r^2(t) \rangle / d \log t = 2$ , then it crosses over to a subdiffusive regime with  $\alpha < 1$ , and eventually enters the Fickian regime with  $\alpha = 1$ . We estimate that the crossover from ballistic to thermal motion ends at the inflection point of  $\alpha$  vs  $\log t$ . The black square in the inset in Fig. 1 indicates the end of the crossover at  $\tau^* \approx 30\tau$  for  $d = 5\sigma$ . A detailed discussion of this criterion for  $\tau^*$  can be found in Supplemental Material [23]. Only  $\langle \Delta r^2(t) \rangle$  for  $t > \tau^*$  is used in the conversion to  $G_{\text{GSE}}(t)$ .

Throughout the Letter, we use  $f = 2$  for the GSE relation, which corresponds to slip NP-polymer boundaries. The slip boundary results from the slip length  $L_s(t)$  being larger than  $d$  for  $t > \tau^*$ . Previous simulations [30] have

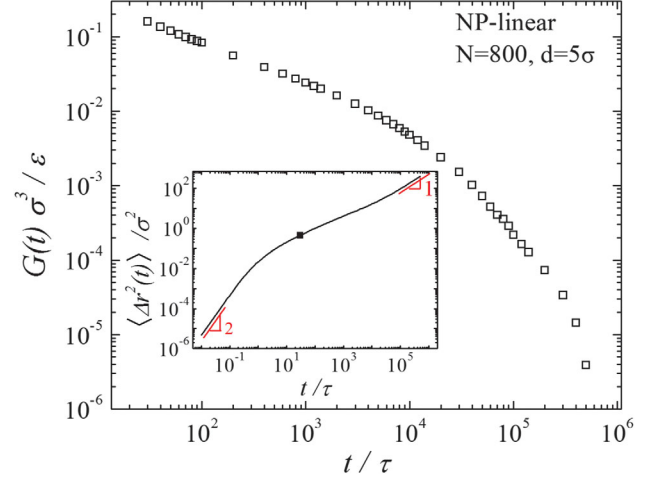


FIG. 1.  $G_{\text{GSE}}(t)$  (open squares) for  $d = 5\sigma$  in linear polymers with  $N = 800$ . The corresponding  $\langle \Delta r^2(t) \rangle$  is shown in the inset (see the black line). The log-log slope  $\alpha = 2$  for the ballistic regime and  $\alpha = 1$  for the Fickian regime are indicated. The estimated end of the crossover between ballistic and thermal motion is indicated by the black square.

demonstrated that  $L_s$  for a bulk polymer melt scales linearly with the melt viscosity  $\eta$ . To estimate  $L_s(t)$  in the present simulations, a similar scaling relation  $L_s(t) \approx b[\eta(t)/\eta_0]$ , in which monomer size  $b \approx \sigma$  and monomeric viscosity  $\eta_0 \approx \tau k_B T / \sigma^3$ , is used. In Supplemental Material [23], we estimate  $\eta(t)$  from  $\int_0^t G_{\text{GK}}(t') dt'$  and demonstrate that the condition  $L_s(t) > L_s(\tau^*) > d$  for  $t > \tau^*$  is satisfied in all simulated NP-polymer systems (see Fig. S1), justifying the slip NP-polymer boundaries.

Results for  $G_{\text{GK}}(t)$  and  $G_{\text{GSE}}(t)$  for linear polymers are shown in Fig. 2(a). For  $G_{\text{GK}}(t)$ , there is first a power-law decay, then the development of an entanglement plateau, and finally the regime of terminal relaxation. At  $t \approx 6.5 \times 10^4 \tau$  with the smallest log-log slope  $|-d \log G(t) / d \log t| \approx 0.07$ ,  $G(t) \approx 2.6 \times 10^{-2} \epsilon / \sigma^3$ , which is close to the theoretical prediction [31] of the entanglement plateau  $G_e \approx 4\rho k_B T / 5N_e \approx 2.5 \times 10^{-2} \epsilon / \sigma^3$  with melt density  $\rho = 0.89\sigma^{-3}$  and  $N_e \approx 28$ . The power-law decrease can be described using the Rouse modes of short unentangled sections of polymer and is predicted to scale as  $G(t) \sim t^{-1/2}$  [32]. The entanglement plateau has been successfully understood based on the phenomenological tube model [31,32], in which entangled chains are confined in their respective tubes with an average diameter  $\approx a$ . For  $Z = N/N_e \approx 30$  as in the present simulations, dynamic processes such as Rouse-type relaxation along the tube, tube length fluctuation and constraint release contribute to the partial stress relaxation prior to the terminal relaxation [33] and result in the deviation of the plateau from a horizontal line. To compare the simulation data of  $G_{\text{GK}}(t)$  with theories for polymer stress relaxation, we fit  $G_{\text{GK}}(t)$  to the theoretical expression proposed by Likhtman

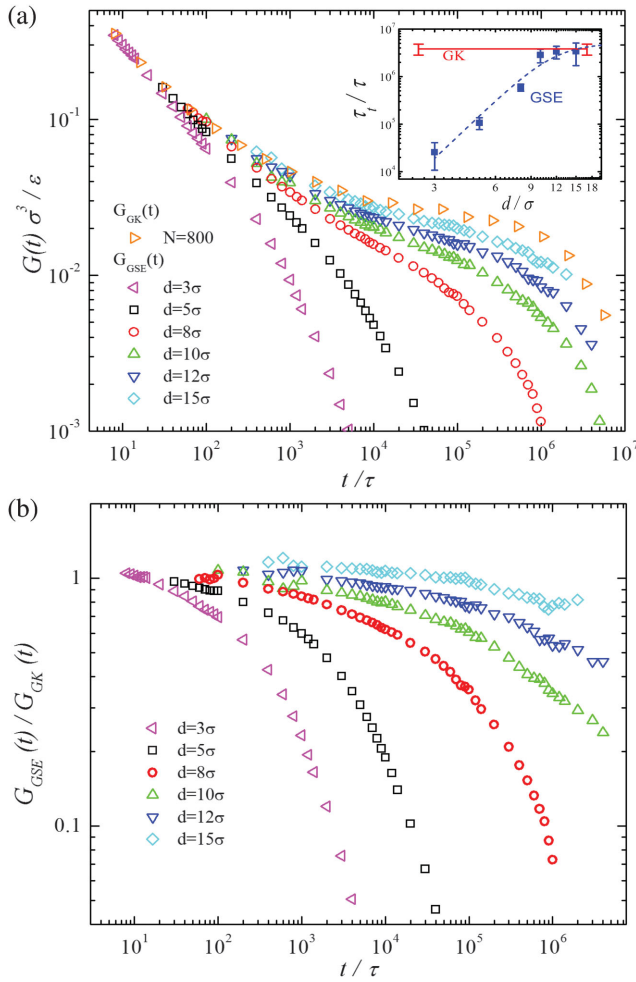


FIG. 2. (a)  $G_{\text{GSE}}(t)$  for NPs with different  $d$  in linear polymers with  $N = 800$  compared to  $G_{\text{GK}}(t)$  for the pure linear polymer melt. The inset shows  $\tau_t$  vs  $d$  for  $G_{\text{GSE}}(t)$  (blue squares) and  $\tau_t$  for  $G_{\text{GK}}(t)$  (red line) with error bars. The dashed blue line indicates the best fit to the scaling theory prediction [15]. (b) The ratio  $G_{\text{GSE}}(t)/G_{\text{GK}}(t)$  for the same systems as in (a).

and McLeish [33]. The details of the fitting are presented in Supplemental Material [23]. The parameters of the best fit are  $N/N_e = Z = 33 \pm 1$ ,  $N_e = 24 \pm 1$ ,  $\tau_e = (1.9 \pm 0.1) \times 10^3 \tau$ , and  $G_e = (0.030 \pm 0.002) \epsilon / \sigma^3$ .

The melt viscoelasticity that affects the thermal NP motion in linear chains depends on  $d$ , as demonstrated in the  $d$  dependence of  $G_{\text{GSE}}(t)$  in Fig. 2(a). For  $d = 3\sigma < a$  and  $d = 5\sigma \approx a$ , there is no plateau in  $G_{\text{GSE}}(t)$ . The dynamic modes of local chain segments that control the motion of NPs with  $d \leq a$  contribute to  $G_{\text{GSE}}(t)$ . The degree of coupling between NP motion and these dynamic modes is quantified by the ratio  $G_{\text{GSE}}(t)/G_{\text{GK}}(t)$  [see Fig. 2(b)]. As  $t$  increases,  $G_{\text{GSE}}(t)/G_{\text{GK}}(t)$  drops below 1, indicating a reduced degree of coupling between NP motion and the corresponding dynamic modes. The decrease of  $G_{\text{GSE}}(t)/G_{\text{GK}}(t)$  is less rapid for  $d = 5\sigma$  than for  $d = 3\sigma$ , indicating stronger coupling between NP motion and the melt viscoelasticity with increasing  $d$ .

Scaling theory [14] predicts that the motion of a NP with  $d < a$  is coupled to the Rouse modes of chain segments with sizes up to  $d$ . Motivated by the theory, we compare  $G_{\text{GSE}}(t)$  for  $d \leq a$  with

$$G(t) = \frac{\rho k_B T}{N} \sum_{p=p_c}^N \exp\left(-\frac{2tp^2}{\tau_R}\right), \quad (3)$$

which is the sum of the modes with Rouse time  $\tau_R$  and mode indices  $p_c \leq p \leq N$ .  $N = 800$ , and  $N/p_c$  is the number of monomers in the largest chain segment that affects NP motion. The comparison is presented in Supplemental Material [23].

As  $d$  exceeds  $a$ , a plateau regime emerges as indicated by the inflection in the log-log plot of  $G_{\text{GSE}}(t)$ . The presence of a plateau means that NPs with  $d > a$  are affected by the confinement of the entanglement network. The confinement is stronger for larger  $d$ , and the coupling between NP motion and melt viscoelasticity is enhanced with increasing  $d$ , as shown in Fig. 2(b). However, for the largest  $d = 15\sigma$ , the coupling is still not complete with  $G_{\text{GSE}}(t)/G_{\text{GK}}(t) < 1$ . We fit  $G_{\text{GSE}}(t)$  for  $d > a$  to the Likhtman-McLeish expression [33] [Eq. (S1)]. As shown in Supplemental Material [23], the best-fit value of the number of entanglements per chain  $Z$  increases with  $d$  but stays below  $Z = 33$  for the bulk melt. The reason for the partial coupling for  $8\sigma \leq d \leq 15\sigma$  has been attributed to the hopping diffusion [13,15] for  $d$  moderately larger than  $a$ .

The terminal regime of  $G(t)$  in Fig. 2(a) is fit to an exponential decay with  $G(t) \sim \exp(-t/\tau_t)$ , where  $\tau_t$  is the characteristic decay time. While  $\tau_t$  characterizes terminal stress relaxation in the pure melt,  $\tau_t$  for  $G_{\text{GSE}}(t)$  is essentially the terminal diffusion time of NP motion. The results of  $\tau_t$  for  $G_{\text{GSE}}(t)$  and  $G_{\text{GK}}(t)$  are shown in the inset in Fig. 2(a).  $\tau_t$  for  $G_{\text{GSE}}(t)$  increases with  $d$  and then saturates around  $\tau_t$  for  $G_{\text{GK}}(t)$  as  $d$  exceeds  $10\sigma$ . Despite the saturation of  $\tau_t$ ,  $G_{\text{GSE}}(t)$  is still below  $G_{\text{GK}}(t)$  for  $d \geq 10\sigma$ . This suggests that NPs with  $d \geq 10\sigma$  are coupled to the melt dynamics up to the longest terminal relaxation mode, though the coupling is not complete. Scaling theory [15] predicts that  $\tau_t \sim d^4$  for  $d < a$ ,  $\tau_t \sim \exp(d/a)$  for hopping diffusion, and finally  $\tau_t$  saturates at the terminal relaxation time of the melt in the large  $d$  limit. The best fit of the  $d$  dependence of  $\tau_t$  to an analytical function motivated by the theory is shown by the dashed line in the inset in Fig. 2(a). Details about the fitting and the terminal regimes are in Supplemental Material [23].

Results of  $G_{\text{GK}}(t)$  and  $G_{\text{GSE}}(t)$  for ring polymers are shown in Fig. 3. Unlike  $G_{\text{GK}}(t)$  for linear polymers,  $G_{\text{GK}}(t)$  for ring polymers has no entanglement plateau, as there is no long-lived entanglement network [34]. As  $d$  increases,  $G_{\text{GSE}}(t)$  for NPs in rings approaches  $G_{\text{GK}}(t)$  for pure rings, and the ratio  $G_{\text{GSE}}(t)/G_{\text{GK}}(t)$  deviates from 1 less rapidly with increasing  $t$  (see the inset in Fig. 3). These results show that NP motion is coupled to the melt viscoelasticity

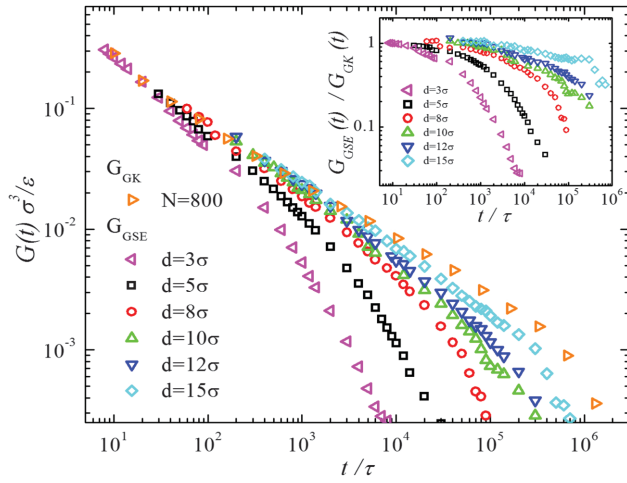


FIG. 3.  $G_{\text{GSE}}(t)$  for NPs with different  $d$  in ring polymers with  $N = 800$  compared to  $G_{\text{GK}}(t)$  for the pure linear polymer melt. The inset shows the ratio  $G_{\text{GSE}}(t)/G_{\text{GK}}(t)$ .

over a wider spectrum of relaxation modes with increasing  $d$ , and the coupling is stronger for larger  $d$ . Scaling theory [13] predicts that NP motion is coupled to the dynamics of ring sections with sizes up to  $d$ , which is smaller than the size of an entire ring polymer.

The motion of NPs with sufficiently large  $d$  is expected to be completely coupled to the terminal relaxation of the polymer melt, and the corresponding  $G_{\text{GSE}}(t)$  excluding the early-time part affected by NP inertia is expected to agree with  $G_{\text{GK}}(t)$  [35]. Previously, based on the examination of the  $d$  dependence of the diffusion coefficient  $D$  for the same simulations [13], we estimated that the Stokes-Einstein (SE) relation  $D = k_B T / 2\pi\eta d$ , where  $\eta$  is the melt viscosity, is recovered for  $d > d_c \approx 20\sigma$  in NP-linear systems ( $N = 800$ ) and for  $d > d_c \approx 30\sigma$  in NP-ring systems ( $N = 800$ ). Since the recovery of the SE relation corresponds to a complete coupling between NP diffusion and the melt viscoelasticity, we expect that the threshold NP size  $d_c$  for the agreement between  $G_{\text{GSE}}(t)$  and  $G_{\text{GK}}(t)$  is also  $20\sigma$  and  $30\sigma$  for NP-linear and NP-ring systems ( $N = 800$ ), respectively.

The important length scale that determines the agreement between  $G_{\text{GSE}}(t)$  and  $G_{\text{GK}}(t)$  differs for NPs in linear and ring polymers. According to the hopping diffusion model [15] for NPs in entangled linear polymers, the hopping probability decreases as  $\sim \exp(-d/a)$ . Hopping diffusion is suppressed for  $d$  sufficiently larger than  $a$ , and therefore the NP motion is completely coupled to the relaxation of the entanglement network even for  $d$  smaller than the size of linear chains. In the present simulation, the estimated  $d_c \approx 4a$  for the complete coupling between NPs and linear polymers. By contrast,  $d$  is compared with the average spanning size  $\langle R^2 \rangle^{1/2}$  of ring polymers to determine the agreement between  $G_{\text{GSE}}(t)$  and  $G_{\text{GK}}(t)$ . As there is no long-lived entanglement network to confine NPs in ring

polymers, the NP motion is increasingly coupled to ring dynamics at longer time scales and larger length scales as  $d$  increases towards  $\langle R^2 \rangle^{1/2}$ . In the present simulations,  $\langle R^2 \rangle^{1/2} \approx 15\sigma$ , and the estimated  $d_c \approx 2\langle R^2 \rangle^{1/2}$  for the coupling between NPs and the entire relaxation dynamics of rings.  $d_c \approx 2\langle R^2 \rangle^{1/2}$  results from the broad distribution of  $R$  around the average  $\langle R^2 \rangle^{1/2}$ . Our analysis in Supplemental Material [23] shows that 33% of all  $R$  are larger than  $\langle R^2 \rangle^{1/2}$ , while almost all (99%)  $R$  are smaller than  $d = 2\langle R^2 \rangle^{1/2}$ . This explains why NPs with  $d = 15\sigma$  are not completely coupled to the entire ring dynamics, whereas NPs with  $d > 2\langle R^2 \rangle^{1/2}$  are anticipated to be almost completely coupled.

Another important length scale for NP-polymer coupling is the slip length  $L_s$  at NP-polymer boundaries. The present simulations correspond to a slip boundary condition with  $L_s > d$ . If  $d > L_s$ , the boundary condition becomes stick. There would be a scaling regime where the NP motion is fully coupled to all relaxation modes of polymers but with stick NP-polymer boundaries. Figure S9 [23] shows the scaling theory prediction for such a regime depending on  $d$  and the polymer size. The existence of two length scales  $d_c$  and  $L_s$  suggests a two-stage coupling of NPs to the entire polymer dynamics with increasing  $d$ . NPs are first coupled to all relaxation modes with slip NP-polymer boundaries as  $d$  exceeds  $d_c$ . Subsequently, the boundary conditions change from slip to stick as  $d$  further increases above  $L_s$ .

In summary, on the basis of molecular simulations, we compare the stress relaxation moduli  $G_{\text{GSE}}(t)$  converted from NP MSD through the generalized Stokes-Einstein relation and  $G_{\text{GK}}(t)$  for pure entangled polymer melts calculated using the Green-Kubo formula. The deviation of  $G_{\text{GSE}}(t)$  from  $G_{\text{GK}}(t)$  results from the incomplete coupling of NP motion to the relaxation modes of the polymer melt. The threshold NP size  $d_c$  for the agreement between  $G_{\text{GSE}}(t)$  and  $G_{\text{GK}}(t)$  is compared to the entanglement mesh size for NP-linear systems whereas to the polymer size for NP-ring systems in which there are no long-lived entanglement networks. Our simulations correspond to slip NP-polymer boundaries, but a change from slip to stick boundaries as  $d$  increases above the slip length  $L_s$  is anticipated. NP-polymer coupling with increasing  $d$  is proposed to be a two-stage process depending on  $d_c$  and  $L_s$ . Our study should help extend the well-established microrheology procedures to nanorheology, which would advance the study of local viscoelasticity that controls the dynamics of nanoscale objects in a viscoelastic medium, such as NPs in polymer nanocomposites and NP-based drug carriers in living cells.

M. R. acknowledges financial support from the National Science Foundation under Grants No. DMR-1309892, No. DMR-1436201, and No. DMR-1121107, the National Institutes of Health under Grants No. P01-HL108808, No. R01-HL136961, and No. 1UH2HL123645, and the

Cystic Fibrosis Foundation. This research used resources at the National Energy Research Scientific Computing Center, which is supported by the Office of Science of the United States Department of Energy under Contract No. DE-AC02-05CH11231. This work was performed, in part, at the Center for Integrated Nanotechnologies, an Office of Science User Facility operated for the U.S. Department of Energy (DOE) Office of Science. Sandia National Laboratories is a multi-mission laboratory managed and operated by National Technology and Engineering Solutions of Sandia, LLC, a wholly owned subsidiary of Honeywell International, Inc., for the U.S. Department of Energy's National Nuclear Security Administration under Contract No. DE-NA-0003525.

\*Corresponding author.  
mr@unc.edu

†Present address: Department of Mechanical Engineering and Materials Science, Duke University, Durham, North Carolina 27708, USA.

- [1] T. M. Squires and T. G. Mason, *Annu. Rev. Fluid Mech.* **42**, 413 (2010).
- [2] T. G. Mason and D. A. Weitz, *Phys. Rev. Lett.* **74**, 1250 (1995).
- [3] B. R. Dasgupta, S. Y. Tee, J. C. Crocker, B. J. Frisken, and D. A. Weitz, *Phys. Rev. E* **65**, 051505 (2002).
- [4] J. H. van Zanten, S. Amin, and A. A. Abdala, *Macromolecules* **37**, 3874 (2004).
- [5] A. C. Balazs, T. Emrick, and T. P. Russell, *Science* **314**, 1107 (2006).
- [6] J. T. Kalathi, G. S. Grest, and S. K. Kumar, *Phys. Rev. Lett.* **109**, 198301 (2012).
- [7] J. Szymanski, A. Patkowski, A. Wilk, P. Garstecki, and R. Holyst, *J. Phys. Chem. B* **110**, 25593 (2006).
- [8] H. Guo, G. Bourret, R. B. Lennox, M. Sutton, J. L. Harden, and R. L. Leheny, *Phys. Rev. Lett.* **109**, 055901 (2012).
- [9] C. A. Grabowski and A. Mukhopadhyay, *Macromolecules* **47**, 7238 (2014).
- [10] R. Mangal, S. Srivastava, S. Narayanan, and L. A. Archer, *Langmuir* **32**, 596 (2016).
- [11] J. Liu, D. Cao, and L. Zhang, *J. Phys. Chem.* **112**, 6653 (2008).
- [12] J. T. Kalathi, U. Yamamoto, K. S. Schweizer, G. S. Grest, and S. K. Kumar, *Phys. Rev. Lett.* **112**, 108301 (2014).
- [13] T. Ge, J. T. Kalathi, J. D. Halverson, G. S. Grest, and M. Rubinstein, *Macromolecules* **50**, 1749 (2017).
- [14] L. H. Cai, S. Panyukov, and M. Rubinstein, *Macromolecules* **44**, 7853 (2011).
- [15] L. H. Cai, S. Panyukov, and M. Rubinstein, *Macromolecules* **48**, 847 (2015).
- [16] J. D. Halverson, W. B. Lee, G. S. Grest, Y. A. Grosberg, and K. Kremer, *J. Chem. Phys.* **134**, 204904 (2011).
- [17] J. D. Halverson, W. B. Lee, G. S. Grest, Y. A. Grosberg, and K. Kremer, *J. Chem. Phys.* **134**, 204905 (2011).
- [18] K. Kremer and G. S. Grest, *J. Chem. Phys.* **92**, 5057 (1990).
- [19] P. J. in't Veld, S. J. Plimpton, and G. S. Grest, *Comput. Phys. Commun.* **179**, 320 (2008).
- [20] R. Everaers, S. K. Sukumaran, G. S. Grest, C. Svaneborg, A. Sivasubramanian, and K. Kremer, *Science* **303**, 823 (2004).
- [21] H.-P. Hsu and K. Kremer, *J. Chem. Phys.* **144**, 154907 (2016).
- [22] T. Ge, M. O. Robbins, D. Perahia, and G. S. Grest, *Phys. Rev. E* **90**, 012602 (2014).
- [23] See Supplemental Material at <http://link.aps.org/supplemental/10.1103/PhysRevLett.120.057801> for details of MD simulation, discussion of the characteristic time  $\tau^*$  at the end of the crossover from ballistic to thermal motion of NPs, estimate of slip length  $L_s(t)$ , fit of  $G_{GK}(t)$  to theoretical expressions, comparison of  $G_{GSE}(t)$  and analytical functions, details about terminal regime of  $G(t)$ , distribution of ring polymer size  $R$ , and theory of two-stage NP-polymer coupling.
- [24] W. B. Lee and K. Kremer, *Macromolecules* **42**, 6270 (2009).
- [25] T. G. Mason, *Rheol. Acta* **39**, 371 (2000).
- [26] The effects of the inertia of both probe particle and viscoelastic medium on particle-based passive rheology have been examined in recent theoretical [27] and computational [28,29] work.
- [27] T. Indei, J. D. Schieber, A. Córdoba, and E. Pilyugina, *Phys. Rev. E* **85**, 021504 (2012).
- [28] M. Karim, S. C. Kohale, T. Indei, J. D. Schieber, and R. Khare, *Phys. Rev. E* **86**, 051501 (2012).
- [29] M. Karim, T. Indei, J. D. Schieber, and R. Khare, *Phys. Rev. E* **93**, 012501 (2016).
- [30] N. V. Priezjev and S. M. Troian, *Phys. Rev. Lett.* **92**, 018302 (2004).
- [31] M. Doi and S. F. Edwards, *The Theory of Polymer Dynamics* (Clarendon, Oxford, 1986).
- [32] M. Rubinstein and R. H. Colby, *Polymer Physics* (Oxford University, New York, 2003).
- [33] A. E. Likhtman and T. C. B. McLeish, *Macromolecules* **35**, 6332 (2002).
- [34] M. Kapnistos, M. Lang, D. Vlassopoulos, W. Pyckhout-Hintzen, D. Richter, D. Cho, T. Chang, and M. Rubinstein, *Nat. Mater.* **7**, 997 (2008).
- [35]  $G_{GK}(t)$  for a NP-polymer composite with the volume fraction of NPs  $\approx 10\%$  differs from  $G_{GK}(t)$  for a pure polymer melt. As a result, a strict comparison should be made between  $G_{GSE}(t)$  and  $G_{GK}(t)$  for the corresponding composite.